Astron. Astrophys. 324, 1105–1114 (1997)

ASTRONOMY
AND
ASTROPHYSICS

Local interstellar cloud electron density from magnesium and sodium ionization: a comparison⋆

R. Lallement[1] **and R. Ferlet**[2]

[1] Service d'Aéronomie du CNRS, BP 3, F-91371 Verrières-le-Buisson, France
[2] Institut d' Astrophysique de Paris, CNRS, France

Received 3 May 1996 / Accepted 2 December 1996

Abstract. The ambient interstellar plasma density (i.e. the plasma density of the interstellar medium surrounding the Sun) directly governs the structure and the size of our heliosphere. Information on this density can be derived from the ionization states of the interstellar species which can be detected in absorption along the paths to the nearby stars, and which can be shown to belong to the Local Interstellar Cloud (LIC). Echelle spectra around the resonance lines of neutral and singly ionized magnesium have been obtained for the nearby star δ Cas with the Goddard High-Resolution Spectrograph (GHRS) on board the Hubble Space Telescope. While apparently a unique velocity component (a unique cloudlet) is detected in both lines of the MgII $\lambda\lambda$2800 resonance doublet, at the expected Doppler shift for the LIC, an extremely small $\lambda\lambda$2853 Mg line is also detected at a Doppler shift compatible with the LIC motion, allowing a measurement of the LIC MgII/MgI ratio, here found to be 400 (-130,+190). This ratio implies a mean electron density of about 0.28 (-0.14, +0.34) cm^{-3} along this line-of-sight, if equilibrium conditions prevail, and if T=7000K, when using the most recent recombination and charge-exchange rates. This MgII/MgI ratio is larger than for Sirius (R$\simeq$220), which lies at 110° from δ Cas, providing some evidence for an ionization gradient in the local cloud. Such an electron density implies a surprisingly large ionization degree, and the upper range of the interval is incompatible with the minimum size of our heliosphere.

A second and independent way to derive the electron density along the path to δ Cas uses the simplicity of the LIC geometry in the sky region surrounding the star, which allows an estimate of the H column-density to the star, as well as previous ground-based CaII data, and the measured NaI/CaII ratio and calcium depletion in the LIC. The resulting most probable electron density at 7000K, 0.05 cm^{-3}, provides a new evidence for a significant ionization degree of the LIC, but is a factor of four to five smaller than the value based on magnesium. The upper limit of 0.19 cm^{-3} remains consistent with the minimum size of our heliosphere. The existence of a common interval to the two determinations: n_e=0.14-0.19 cm^{-3} implies that ionization equilibrium within the LIC is not totally precluded. However, the lack of a real convergence deserves further observations, involving other interstellar species. The common interval is compatible with the result of Frisch (1994), from anomalous C and O cosmic rays abundances, if carbon is not too much filtered at the heliospheric interface. On the other hand, the sodium-based most probable value is in agreement with neutral hydrogen deceleration at the heliospheric interface for the Baranov two-shocks model, as well as with the ionization degree of hydrogen implied by local EUV sources.

Key words: stars: δ Cas – ISM: atoms – ISM: general – interplanetary medium – solar neighbourhood

1. Introduction

There is a growing interest for the determination of the actual value of the ionization degree of the extra-heliospheric interstellar gas, i.e. the region of the local interstellar cloud the Sun is traveling through. This interest is linked to the possibility for the Voyager 1 and 2 spacecraft, now at $\simeq$50 and $\simeq$60 AU respectively, to cross the heliospheric interface early enough (before 2020) to provide information on the location and the structure of this interface, and maybe to probe for the first time the interstellar space directly "in situ". As a matter of fact, the local interstellar plasma pressure (in addition to the magnetic and cosmic rays plasma pressure) directly influences the distance to the heliospheric interface which separates the solar wind from the local interstellar medium, and in general the size of our heliosphere. Assuming that the solar wind confinement is mainly due to the thermal interstellar plasma, pressure balance calculations show that the crossing should occur before 2020, provided the interstellar H^+ ($\simeq e^-$) density is as large as 0.1 cm^{-3}, i.e. comparable or equal to the neutral H density. Information on the local cloud interstellar plasma density can be brought by spectroscopic studies of the local interstellar medium at very high

Send offprint requests to: R. Lallement

⋆ Based on observations with the NASA/ESA Hubble Space Telescope, obtained at the Hubble Space Telescope Science Institute which is operated by the association of Universities for research in Astronomy Inc., under NASA contract NAS5-26555

resolution, through the detection of the local gas absorption lines in the spectra of nearby stars. Such studies have been performed for many years in the visible (e.g. Hobbs 1975, 1976, Ferlet et al. 1986, Lallement et al. 1986, Lallement 1990, Hobbs and Welty 1991, Welsh et al. 1991, Crawford, 1991, Vallerga et al. 1993), and in the UV with Copernicus and IUE (e.g. Vidal-Madjar et al. 1978, MacClintock et al. 1978, Frisch 1981, Frisch and York 1983, Bruhweiler et al. 1984, Landsman et al. 1986, Molaro et al. 1986, Murthy et al. 1987, Genova et al. 1990). More recently very high resolution (R$\simeq$100,000) and high quality UV observations have been made possible with the Goddard High Resolution Spectrometer (GHRS) on board the Hubble Space Telescope (HST). This instrument also allows a precise wavelength scale calibration (commonly $\simeq$ 1.5 kms^{-1} in the Echelle mode).

The local gas within 20 pc has a complex dynamical structure, with small "cloudlets" or pieces of clouds of size of the order of a parsec having bulk motions differing by 5-10 kms^{-1} (Linsky et al., 1995 and references above), forming the so-called "Local Fluff". The closest gas or Local Interstellar Cloud (hereafter LIC) produces very small absorption lines in the nearby stars spectra which have been identified by using the Doppler triangulation method on visible data (Lallement and Bertin 1992 (herafter LB92), Bertin et al. 1993b, Lallement et al. 1995) allowing the determination of its velocity vector. This vector has been confirmed both by Hubble GHRS observations (Linsky et al. 1993, Lallement et al. 1994 (hereafter LBFVB), Lemoine et al. 1996, Linsky et al. 1995), and in a completely different way by the direct detection on board the interplanetary spacecraft Ulysses of the interstellar neutral helium atoms in the solar system, found by Witte et al. (1993) to also flow at the same velocity. For a detailed chronology and description, see Lallement et al., 1995. This cloud, the LIC, is moving at 26 $\pm$ 1 kms^{-1} (heliocentric velocity) from l_{II}=(6 $\pm$ 3)°, b_{II}= (16 $\pm$ 3)°, or α= 254.5°, δ= -15°. The temperature of the cloud is around 7000 K as measured from the Capella deuterium line (Linsky et al. 1993, 1995) and the solar system helium distribution (Witte et al. 1993). A second colder cloud, moving at a slightly different velocity (29 kms^{-1} and about 3° from the LIC vector), is also found to be present in the close vicinity of the Sun (Lallement et al. 1990, Linsky and Wood 1996). It is not clear whether or not this material, detected towards galactic longitudes comprised between -110° and +45°, is simply an extension of the LIC, or is separated from it by hot gas of the Local Bubble. There are at least four other clouds than these two within 5 pc, as show the Altaïr (Ferlet et al. 1986, Lallement et al. 1995), Sirius (LBFVB) and Procyon (Linsky et al. 1995) GHRS spectra, which all three exhibit at least two absorption lines. A small neutral magnesium (MgI) absorption line has been detected towards Sirius at the LIC Doppler shift along with absorptions by MgII (and other species). The MgII/MgI ionization balance was used by LBFVB to infer the LIC electron density, under the assumption of ionization equilibrium. The surprisingly large value of the resulting electron density has raised some doubts about the identification of the small spectral feature as due to MgI (LBFVB), and a confirmation of the detection and of the MgI/MgII ratio was needed.

The ionization state of the nearby gas in general is a long-standing question (Cox and Reynolds 1987). The dispersion measure for the closest pulsar (130 pc) corresponds to an average electron density of 0.02 cm^{-3} (Reynolds, 1990). Recently EUV observations of nearby white dwarfs have brought new results on the ionization of helium and hydrogen in the Sun vicinity. Vennes et al. (1993) have detected singly ionized helium and shown that helium is in average 25% ionized along the line-of-sight to the nearby white dwarf GD246. Dupuis et al. (1995) have shown that helium is systematically more ionized than hydrogen (HI/HeI around 14) in the local ISM. But, despite the very strong EUV flux detected from ϵ CMa (Vallerga et al., 1993), such a strong ionization of helium can not be due to discrete ionization sources only (Vallerga and Welsh, 1995), but requires a strong EUV diffuse background from the hot gas (Cheng and Bruhweiler 1990) or the conductive interfaces between the local clouds and the hot gas (Slavin 1989), or a recent ($\leq 10^6$ yrs) ionizing event. On the other hand, the EUVE measurements have placed a strong upper limit to the intensity of the diffuse EUV radiation field, making the last hypothesis the most likely (Jelinsky et al. 1995). Also, as discussed by Cheng and Bruhweiler (1988), even with hot gas contribution there are still difficulties when trying to reproduce Hα background intensities (e.g. Reynolds 1987).

The cycle 3 Guest Observer (GO) program P4274 has been devoted to the ionization equilibrium in the LIC. In this program, the nearby star δ Cassiopeiae has been chosen as a target star for reasons which are detailed in Sect. 3, with the aim of determining the Local Cloud electron density, through the measurement of the MgII/MgI abundance ratio. The GHRS data and the profile fitting results are presented in Sect. 2. In Sect. 3 we discuss the local cloud structure and its homogeneity in the sky region around δ Cas, and give an estimate of the HI column density towards this star. Then we use previous ground based observations to derive the mean electron density towards δ Cas in a completely independent way, based on calcium equilibrium and sodium and calcium observations (section 4). We also use sodium and hydrogen columns to estimate the electron density towards Altaïr in the slowest of the three velocity components present along this line-of-sight, which, from Doppler triangulation results, corresponds to either the LIC or the nearby G cloud. In the last section, we compare the different results and their consequences in terms of heliospheric confinement.

2. Neutral and singly ionized magnesium towards δ Cas

2.1. Data

Echelle-B spectra of the nearby star δ Cas (26 pc) have been obtained at a spectral resolution of about 90,000 with the HST-GHRS around the $\lambda\lambda$2800 MgII doublet and the $\lambda\lambda$2853 MgI resonance transitions. In order to maximize the quality of the spectrum, all the GHRS options have been used, namely i) the oversampling mode (four points per resolution element),

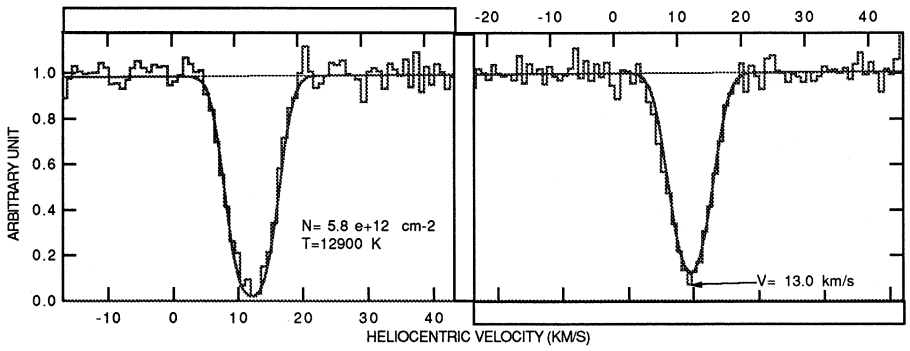

Fig. 1. Echelle spectrum of δ Cas around the MgII lines. For each line of the doublet, the continuum on both sides of the interstellar line has been fitted by a polynomial function, and the spectrum has been divided by the fitted continuum. Both lines of the doublet have been fitted simultaneously for the same densities and temperatures of the absorbing clouds. What is shown is the best-fit to the data with one theoretical cloud (solid line).

ii) the FP-SPLIT procedure which shifts the exposure into sub-exposures at different positions of the grating, providing a way to remove photocathode granularities, and iii) the substepping/COMB procedure which is used to remove diode-to-diode irregularities. The data issued from the standard reduction and calibration "pipeline" were reprocessed with the IRAF routine described by Bertin et al. (1993b), excepted for the "splitting" treatment of the MgI data for which we have encountered particular difficulties (see below). The MgII and MgI exposures lasted 460 and 6300s, resulting in S/N ratios of $\simeq$15 and $\simeq$60 respectively at the bottom of the stellar lines where the interstellar absorption occurs. The need for a better signal to noise for neutral magnesium is due to the extremely small quantity of this species. Wavelength calibration were obtained through a special platinum-lamp exposure after each series of exposures. This has been shown to provide a wavelength precision better than 1.5 kms^{-1} in most cases (Bertin et al. 1993b, LBFVB). This is indeed the case for the two MgII lines. During a typical use of the IRAF routine, individual spectra recorded when the FP-SPLIT procedure is activated are shifted according to their relative offsets before being co-added. The offsets are calculated by means of cross correlations of the spectra two by two. In the case of the MgI spectrum, offsets calculated in this way were slightly different from those coming out from the pipeline. A possible reason is the lack of sharp features in the MgI spectral region, which makes the cross-correlation unprecise. The comparison between the two methods showed that in the final spectrum a given feature can be found at locations differing by at least 3 or 4 sub-pixels (here quarters of pixels), depending on which method is used. So instead of using the results of the cross-correlations we have used the pipeline values, considering however that accuracy of the wavelength calibration is somewhat decreased. We have estimated for this MgI spectrum an additional uncertainty of $\simeq$0.7 pixel (about 2 kms^{-1}), and then a total error of 3.5 kms^{-1} instead of the usual 1.5 kms^{-1}. We will come back to this point in the next section.

The choice of δ Cas as a preferential target is due to its location at a distance and in a sky region such that we were expecting only one absorption, the one due to the Local Cloud (see Sect. 3).

Figs. 1 and 2 show enlarged portions of the spectra around

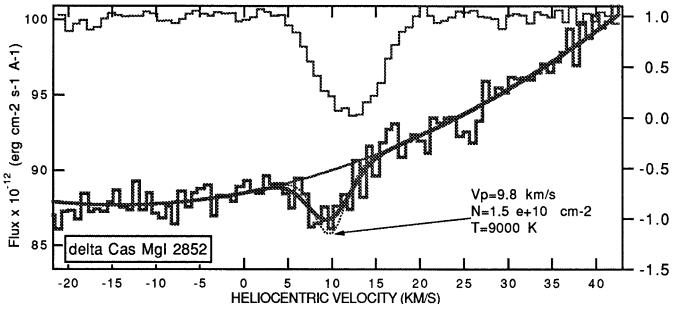

Fig. 2. The Echelle spectrum around the $\lambda\lambda$2853A MgI line and the best-fit theoretical profile for a single absorbing cloud. The strongest line of the MgII doublet has been plotted on top in the same heliocentric frame.

the two MgII lines and the $\lambda\lambda$2853 MgI line. Apparently a single velocity component is detected for the three transitions.

2.2. *Profile-fitting results*

Theoretical profiles have been obtained for the three lines, assuming a single cloud is present. The profile-fitting program is described in LB92. Atomic data are taken from the compilation by Morton (1991), and the instrumental function is from the GHRS handbook (Duncan, 1992). The parameters characterizing the cloud (column-density N, velocity, b-value or apparent temperature) are free and independent parameters during the fitting procedure, except for the two lines of the MgII doublet fitted simultaneously with the same N and the same b value. Fig. 1 shows the theoretical profiles resulting from the adjustment to the data superimposed on the spectrum. The MgII interstellar line centers are found at heliocentric velocities of 12.0 $\pm$ 1.5 kms^{-1} and 13.0 $\pm$ 1.5 kms^{-1} respectively for the two lines of the doublet, in excellent agreement with the expected Doppler shift for the LIC (LB92, Bertin et al., 1993b) of 13.0 kms^{-1}, and the Doppler-shift of the CaII line detected in the visible of 12.9 kms^{-1} (LB92). The derived apparent temperature is 12,900K $\pm$ 2500K (b= 3.0 kms^{-1}), i.e. slightly larger than the apparent temperature of the LIC component towards Sirius (about 10,500K). In the case of Sirius, both the turbulent and thermal broadening could be determined thanks to the comparison between magnesium and iron line widths. Here we can not apply this procedure,

because we measure only Mg lines. If the true temperature is of the order of 7000K, as for Sirius, and compatible with the local helium temperature measured in situ with Ulysses (Witte et al. 1993), then the turbulent broadening is of the order of 1.9 kms^{-1}, to compare with $\xi \simeq 1.4$ kms^{-1} (LBFVB) towards Sirius and $\xi \simeq$ 1.6-1.7 kms^{-1} towards Capella (Linsky et al. 1993).

The measured MgII column-density is $(5.8 \pm 1.0)\,10^{12}$ cm^{-2} (from the two lines of the doublet), similar to columns measured towards surrounding stars (see Sect. 3). The MgII column-density and apparent temperature are slightly different from the earlier values derived from the best fit of the $\lambda\lambda$2803 line alone ($6.5 \pm 1\ 10^{12}$ cm^{-2} and 12,000K, Lallement et al. 1995). This is due to the additional constraints linked to the simultaneous adjustments to the two lines of the doublet. The signal to noise ratio of $\simeq$60 for the bottom of the MgI ($\lambda\lambda$2853) stellar line is good enough to detect a MgI absorption line, probably the counterpart to the MgII absorption. The line center is found at 9.8 ± 3.5 kms^{-1}, if we consider the unusually large uncertainty discussed in the previous section. This range includes the MgII line velocity of 12.5 ± 1.5 kms^{-1}, and the expected location at 13.0 kms^{-1}. The linewidth of the MgI line is found to correspond to an apparent temperature of 11,500 (+8000K,-5000K). This determination is very uncertain due to the noise, and we can only say that the agreement with the apparent temperature linked to the MgII is not ruled out, and that such a range precludes a hot or cold medium as being the source of the absorption, which plays in favor of the same medium being sampled by the two species.

Despite the apparent discrepancy between the central values for the velocity shifts for MgII and MgI, we believe that these two lines indeed do sample the same cloud. As a matter of fact, neutral magnesium is permanently created by Mg^+ recombination. For all previous HST observations of the very close gas (Linsky et al. 1993, LBFVB, Lallement et al. 1995, Lemoine et al. 1995, Linsky et al. 1995), species which are associated with predominantly neutral and ionized regions are found at the same velocities, in favor of a partially ionized medium.

If we suppose that the neutral magnesium line Doppler shift is different from the MgII line Doppler shift, then we have to consider the two following cases: a) MgII and MgI belong to two different clouds. This implies that MgI is the dominant form in one of the two clouds, and that this particular cloud is completely shielded from the ambient UV field. This requires a very high volumic density and a much stronger column-density in comparison with the small amount of detected magnesium. As a conclusion, this situation is extremely unlikely. b) There are two MgII clouds whith radial velocities separated by 1 or 2 km s^{-1}, and the neutral magnesium is associated with the slowest of these two clouds. This implies that these two clouds have very different MgI/MgII ratios. The electron density estimate we derive (next section) applies to the first cloud only, after some corrections for the amount of MgII (the MgII column associated to the MgI at 10 kms^{-1} is at least a factor two smaller than the total MgII amount). As we will see, the electron density will become very large for this first cloud. On the contrary, the second, faster cloud, will be found predominantly neutral. This implies the co-existence of a neutral cloud, and a strongly ionized region. Until better observations allow to separate these two masses of gas (if they are real), we will assume in what follows that the MgI and MgII absorptions arise in the same cloud, and that the MgI line actual Doppler shift is identical to the more accurately measured MgII shift, i.e. around 12.5-13.0 kms^{-1}.

The MgI column-density is found to be $1.45 \pm 0.3\ 10^{10}$ atoms cm^{-2}. This is to compare with the MgI column towards Sirius of ($0.75 \pm 0.15\ 10^{10}$ atoms cm^{-2} for the LIC component, LBFVB), while Sirius is located at 100° from δ Cas. This second MgI detection for very close stars makes unlikely the hypothesis that these small lines detected towards Sirius and now δ Cas are stellar features, instead of interstellar lines (a possibility discussed by LBFVB). As a matter of fact, the Doppler shifts of the observed absorptions with respect to the stars are very different for the two targets, precluding now a stellar feature to be responsible for both absorptions. On the contrary the heliocentric Doppler shifts are in good agreement with the projections of the LIC velocity vector towards the two directions. The resulting ratio R= N(MgII)/N(MgI)=$(5.8 \pm 1.0)10^{12}/(1.45 \pm 0.3)10^{10}$ is here found to be R= 400 (-130,+190). The average value is about twice the ratio measured towards Sirius R= 220 (-40,+70), altough the two error intervals are almost contiguous. This gives some evidence that there is a gradient of the ionization ratio within the cloud, but needs confirmation and a better knowledge of the line structure.

2.3. Electron density estimate

The MgII/MgI ratio is directly sensitive to the electron density, provided equilibrium conditions prevail (Bruhweiler et al. 1984, Frisch et al. 1990 (hereafter FWYF), Frisch 1994), through the balance between recombination and ionization. In the case of magnesium, the charge-exchange with the protons $H^+ + Mg \rightarrow H + Mg^+$ acts as an ionization process, in addition to photoionization (Allan et al. 1988), and in the following we will assume that the reverse charge-exchange is negligible in comparison with the direct process. The equilibrium can be written as:

$$n_{MgII} * n_e * \alpha(T) = \gamma_{ph} * n_{MgI} + \sigma_{ex} * n_{HII} * n_{MgI} \qquad (1)$$

where γ and α are the ionization and recombination rates respectively. α is the sum of the dielectronic and direct radiative recombination rates, γ_{ph} is the photoionization rate and σ_{ex} is the proton-neutral magnesium charge-exchange ionization rate. Neglecting the charge-exchange processes is equivalent to omit the last term of Eq. 1. This equation shows that at equilibrium, the neutral magnesium density increases with the number of recombinations, which, for a given temperature, means when the electron density is high enough. The measured ionizing field, within the interval 1300-1620A, leads to $\gamma_{ph} = 0.4 \pm 0.05\ 10^{-10}$ s^{-1} (Phillips, Gondhalekar and Blades 1981). The charge-exchange rate has been calculated by Allan et al. (1988) and found to be approximated by $1.74\ 10^{-9} * \exp(-2.21/t4)$ n(HII), with t4 = T/10^4 K. Assuming n_e= n(HII), Frisch (1994) has calculated which n_e

and T ranges of values do correspond to the equality of the two ionizing processes, i.e. photoionization and charge-exchange, and concludes that the charge-exchange does not have a strong influence. However, very high electron densities are derived here from the observed magnesium equilibrium, both for our previous Sirius data and the present δ Cas data, and the use of Eq. 1 shows that, in this case, charge-exchange is not totally unsignificant. The recombination rate has been calculated by different groups, as discussed by FWYF, and more recently by Frisch (1994). In the Sirius analysis, we have used the results of Jacobs et al. (1979), which are tabulated above 10000K, and which we have extrapolated down to 6500K. We have also neglected radiative recombination. These assumptions lead to α_{diel} = 4 (resp. 6.0, 12.0) 10^{-13} cm^3 s^{-1} at T= 6500 (resp. 7000,8000) K. In a recent study, Frisch (1994) has used the more recent Nüssbaumer and Storey (1986) recombination rates to reestimate the LIC electron density towards Sirius. Nüssbaumer and Storey have recalculated the recombination rates while taking into account auto-ionization in a different way. They come out with a dielectronic recombination rate smaller by about a factor of 1.5 to 2 than the Jacobs et al. (1979) rates. More precisely, these rates, valid at temperatures $\leq$10000K, and then directly applicable to the LIC are α_{diel} = 3.0 (resp. 3.55, 4.71) 10^{-13} cm^3 s^{-1} at T= 6500 (resp. 7000,8000) K. Using the Nüssbaumer and Storey dielectronic recombination rate, and increasing it by the direct radiative rate calculated by Aldrovandi and Péquignot (1973) (the use of a lower dielectronic rate makes the latter direct radiative rate unnegligible in comparison with the former), the total rate becomes 5.5 10^{-13} at T= 7000K. Assuming homogeneity all along the line-of-sight, the volumic densities n(MgII) and n(MgI) in Eq. 1 can be replaced by the column-densities N(MgII) and N(MgI), by multiplying both sides of the equation by the length of the cloud between the Sun and the target. If R= N(MgII)/N(MgI), Eq. (1) becomes

$$n_e = \frac{\gamma_{ph}}{\alpha(T) * R - \sigma_{ex}} \quad (2)$$

where σ_{ex} is zero if one neglects charge-exchange processes. Finally, assuming -i) equilibrium, -ii) a temperature of 7000K, -iii) uncertainties on the ionizing rate of $\pm$ 12.5%, -iv) the Nüssbaumer and Storey rates, the δ Cas ratio R= 400 (-130, +190) is found to correspond to an electron density n$_e$=0.18 (-0.07,+0.12) cm^{-3} if neglecting charge- exchange, and n$_e$=0.28 (-0.14,+0.34) cm^{-3} if including it as described in Eq. (1). More generally, Fig. 3 shows the results for the whole temperature range 6,000-10,000K, with and without charge-exchange. Densities calculated with the Jacobs et al recombination rates are also given for comparison with the Nüssbaumer and Storey rates. Note that the reanalysis of the Sirius data using the above assumptions i) to iv), now leads to n$_e$=0.33 (-0.11,+0.22) cm^{-3} if neglecting charge- exchange, and n$_e$=0.85 (-0.44,+1.35) cm^{-3} if including it.

2.4. Discussion

Such number densities for the electrons derived from magnesium equilibrium are very large (and for Sirius unrealistically large). In the immediate vicinity of the Sun, values above 0.3 cm^{-3} can certainly be excluded. As a matter of fact, the Voyager and Pioneer spacecraft, which are still surrounded by the supersonic solar wind, provide a lower limit to the distance to the termination shock of about 60 AU, which can be converted into an upper limit to the circumsolar electron density. This limit is presently of the order of 0.25- 0.3 cm^{-3} (using heliosphere size estimates by Axford, 1990), i.e. a higher interstellar plasma density would exert a strong enough pressure to confine the solar wind within less than 60 AU, and the spacecraft would have already crossed the solar wind terminal shock. This upper limit becomes even lower if the interstellar magnetic field is actually stronger than the estimated 1.5 μG intensity, and if one takes into account an additional pressure by the cosmic rays and the neutrals coupled to the plasma. Unless the LIC is largely inhomogeneous in density, which is not suggested by observations (see the similarity of the Sirius and δ Cas results, and of the FeII, MgII, H and CaII abundances in the LIC towards all the nearby stars (Lallement et al. 1995), electron densities above this value are precluded, and this raises questions about the above method based on magnesium equilibrium. In the case of Sirius, it has already been pointed out by LBFVB that taking into account the charge-exchange leads to surprisingly large densities if the temperature is as low as 7000K, but now the situation becomes worse with the new recombination rates and the exact treatment through Eq. 1, which imply an even larger electron density. One possible explanation is the existence of significant temperature inhomogeneities along the path to the star. As a matter of fact, our electron density estimates have been done under the assumption of constant temperature along the line-of-sight. Since the dielectronic recombination rate is a strongly increasing function of the temperature, any region warmer than the assumed 7000K could provide relatively more neutral magnesium as compared with other regions. In other words, if the temperature is at some locations larger than the local temperature of 7000K, the actual electron density could be smaller than what is inferred by assuming homogeneity. However, this cannot be a very important effect because the neutral magnesium line is apparently not broader than the MgII line, so only a limited amount of the neutral magnesium is produced in warmer regions. An ionization gradient and a boundary effect may be the most likely explanations for such large densities (LBFVB). This is consistent with the picture of Frisch (1994). The amount of material in the LIC component towards Sirius is the smallest ever detected from UV lines, indicating that the cloud surface is very close in this direction, while in the direction of δ Cas it is four times farther. If the cloud boundary is more ionized than the inner parts, it could explain why the average ionization towards Sirius is found larger than towards δ Cas. In this case, the discrepancy by a factor of $\simeq$2 between the two ratios R= Mg(II)/Mg(I) towards Sirius and δ Cas, which can only marginally be accounted for by the observational errors, provides evidence for such a gradient in the cloud. The gradient has to be rather strong if one considers that what we measure are median values for the MgII/MgI ratios. In any case, only the lower values from the resulting electron density ranges are compatible with the upper limit on the

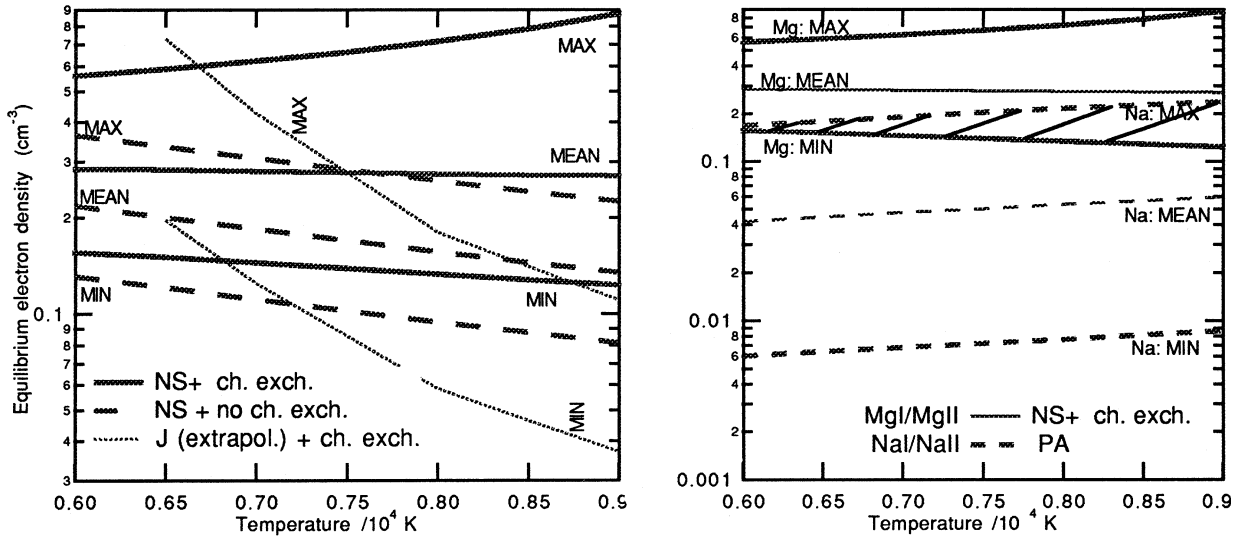

Fig. 3. Left:Most probable, minimum and maximum electron density derived from magnesium equilibrium, as a function of the LIC electron temperature. Solid (resp. dashed) lines correspond to the Nussbaumer and Storey recombination rate with (resp. without) charge-exchange processes taken into account. Dotted lines correspond to minimum and maximum values for the extrapolated Jacobs et al recombination rate. Right: Most probable, minimum and maximum electron density derived from sodium (dashed lines) and magnesium (solid lines) equilibrium. The common interval is shown by hatching.

circumsolar plasma density of $\simeq$0.25 cm^{-3} linked to the observation that the Voyager are still cruising within the supersonic solar wind.

Cheng and Bruhweiler (1990) have calculated the ionization gradient inside diffuse clouds, under the effect of ionizing radiation penetration. They have shown that for a neutral H column density of the order of 10^{18} cm^{-2} and volumic densities of the order of 0.1 cm^{-3}, significant ionization gradients are present over distances of the order of a parsec. But, as pointed out by Vallerga and Welsh (1995), the average ionization ratios derived from magnesium (more than 50%) are hardly compatible with the ambient ionizing field. Both the Cheng and Bruhweiler (1990) models, and their own recent calculations which include the star ϵ Cma, the most powerful ionizing source in the Sun vicinity discovered by the Extreme UltraViolet Explorer, show that 20% ionization of H is the most likely value. We will come back to this point in the last section. The possible existence of two components seen in the MgII line which would be responsible for the Doppler shift gap, if it is real, makes the situation even more difficult to explain in terms of ionization sources. The cloud containing the MgI and only a fraction of the detected MgII will be found to have a very high electron density of more than 0.4 cm^{-3} (if we estimate from Doppler shifts and linewidths that at least half of the MgII belongs to it), while the cloud with no neutral magnesium has to be predominantly neutral.

As a conclusion, the magnesium equilibrium favors large electron densities, maybe irrealistically large. This is why we have tried to make comparisons with other species (next two sections).

3. Neutral H column-density to δ Cas

The reason for having chosen δ Cas as a preferential target for the LIC study is its location inside a particularly simple region, in the geometrical sense, as have shown previous observations, both in the UV and in the visible. For five stars from the LB list, a unique CaII absorption line is detected. These stars are α Cep (15 pc), α Lac (25 pc), δ Cas (27pc), γ Aqr (22 pc) and δ Her (23 pc). The first three are angularly close and have very similar and very low (0.5-1.0 10^{10} cm^{-2}) CaII column-densities, providing evidence that only the LIC is present along these lines-of-sight. This may be true for the last two stars which are located at higher latitudes, but due to their large CaII columns make we suspect blends with other denser and farther clouds (if not, it would be a sign of the LIC elongated towards $l_{II} \simeq$40, $b_{II} \simeq$+30°, see Lallement et al. 1995). The detection of a unique CaII component, does not mean necessarily that UV spectra will also reveal a unique velocity component. The UV spectra are more sensitive to small amounts of gas. But Capella (12 pc), which is angularly close to the portion of sky delimited by these three (or five) targets, was shown by Linsky et al. (1992) to exhibit only one component at the LIC Doppler shift in all strong UV lines. Also, the CaII component which corresponds to the Capella absorptions in the UV can be estimated towards the farther star η Aur (LB) at 5° from Capella, and is found to be 0.7 10^{10} cm^{-2}, i.e. similar to the three other values given above. On the celestial map Capella, α Cep and α Lac form a triangle of 60° basis which center is δ Cas. Thus, for this triangle, there are four "single cloud" cases along L-O-S of 12 to 27 pc, for four coherent Doppler shifts and four similar CaII column- densities (see Table 1), and one of these stars has been observed in the UV and shown to exhibit only one cloud. Consequently, this part of

Table 1. Target galactic longitude and latitudes l_{II} and b_{II}, distance d (pc), N=number of detected velocity components, Vth=theoretical projection of VLIC, Vobs= observed velocity shift, N(MgII,etc..) =column densities of FeII etc.. in units of atoms/ions cm^{-2}, and corresponding references. (*): this work, (1): Ferlet et al. 1986, (2): Linsky et al. 1993, (3): Lallement and Bertin 1992, (4): Lallement et al. 1995, (5) Lemoine et al. 1996. ‡:Column-density of LIC component towards η Aur, at $\simeq 5^\circ$ from α Aur.

Star	l_{II},b_{II} deg	d pc	N	V_{LIC} kms^{-1}	V_{obs} kms^{-1}	N_{MgII} $*10^{12}$	N_{HI} $*10^{18}$	N_{CaII} $*10^{10}$	Ref
δ Her	46.8;31.4	23	1	-19.7	-19.5			3.1	3
α Aql	48.;-9.	5.0	3	-17.2	-17.4	5.0±1.5	—-	0.70	4,1
γ Aqr	62.2;-45.8	22	1	-4.4	-4.5			1.1	3
α Cep	101.0;9.2	15	1	0.9	0.2			0.7	3
α Lac	101.3;-6.6	25	1	3.1	3.5			1.0	3
δ Cas	127;-2	27	1	12.9	12.3	6.0±1.	—-	0.50	*,3
G191-B2B	156;7	48	3	20.3	20.6	5.2±2.0	1.8	—-	5,4
α Aur	162.5;4.5	12.5	1	22.0	23.0	6.5	1.8	0.60‡	2

the sky appears as free of clouds beyond the Local Cloud over distances as large as 25-30 pc. This seems to be a unique situation, since other regions have a more complex velocity structure, with 2,3 or more patches of gas at different velocities (see the cases of Sirius, and Procyon). This is why the high probability of detecting towards δ Cas only the LIC, even in the sensitive UV transitions, had motivated our choice. This is indeed what is observed, i.e. the detection of a unique component in the UV towards δ Cas confirms that towards this part of the sky, the Local Cloud, and only the Local Cloud, is detectable over large distances. In the following we rely on this simple geometry, and the similarity of the LIC column-densities over a 60° region, to argue that the neutral H column-density towards δ Cas can be estimated by comparison with surrounding targets for which H is measured.

Table 1 shows the amounts of LIC ionized magnesium measured with the GHRS towards Capella (12.5 pc) (Linsky et al. 1993), the white dwarf G191-B2B (48 pc) (Lemoine et al. 1996), which has the particularity of being angularly very close to Capella, δ Cas (27 pc) (this work), and Altair (5pc) (Lallement et al. 1995). More precisely, only the absorption line at the exact Doppler shift corresponding to the LIC velocity vector projection onto the star direction is indicated. The larger uncertainty on the column-density in the case of Altair is due to blending, two other clouds than the LIC being present between the Sun and Altaïr. The amount of singly ionized calcium CaII is indicated, when available (Ferlet et al. 1986, Lallement et al. 1986). CaII columns towards α Cep, α Lac and η Aur have been added. For two targets, Capella and G191- B2B, the LIC HI column has been accurately measured, and the results are in rather good agreement (1.71-1.76 and 1.85 10^{18} cm^{-2} from Linsky et al. 1993 and Lemoine et al. 1994 respectively). Table 1 shows that all these results are coherent and favor a rather simple structure towards this part of the celestial sphere. More important, it shows that the CaII/MgII ratios are similar, implying a high level of homogeneity in this limited region of the sky. The CaII abundance being highly sensitive to electron density, at variance with MgII which is the dominant form of this element, this also implies a homogeneous ionization in this portion of the local cloud (as seen in Sect. 2, it may be different towards Sirius). Taking advantage of this rather simple structure and homogeneity, and then assuming a constant (HI+HII)/MgII (or alternatively (HI+HII)/CaII) ratio, we can estimate the HI column on the path to δ Cas, by comparison with Capella (or G191-B2B). It follows, since the Capella and δ Cas MgII columns are both equal to 6.5 10^{12} cm^{-2}:

$$\begin{aligned} N_{H,\delta Cas} &= N_{HI+HII,\delta Cas} \\ &= N_{HI+HII,Cap} * \frac{N_{MgII,\delta Cas}}{N_{MgII,Cap}} \\ &= \frac{1}{1-f} * (1.8 \pm 0.25) 10^{18} cm^{-2} \end{aligned} \quad (3)$$

where f is the fractional ionization towards Capella f= N_{HII}/(N_{HI}+N_{HII}). If the gas is predominantly neutral towards Capella, then f$\simeq$0 and $N_{H,\delta Cas}$ =(1.8 ± 0.25) 10^{18} cm^{-2}.

4. Electron density from calcium and sodium equilibrium

The simultaneous knowledge of CaII and H columns for an individual cloud allows an estimate of the ionization balance of calcium, and then of the electron density responsible for this balance, provided the calcium abundance in the gaseous phase is known. The dominant forms of calcium (resp. sodium) in the gaseous phase are CaII (resp. NaI) and CaIII (resp. NaII), for warm and low density clouds similar to the LIC in the ambient UV field (Pottasch 1972). In these conditions, the total calcium column is

$$N_{Ca} = N_{CaII} + N_{CaIII} = N(H) * (Ca/H)_{SUN} * 10^{\delta} \quad (4)$$

if δ is the calcium depletion. N_{CaIII} can be calculated as a function of N_H and N_{CaII}, and the electron density is given by the calcium equilibrium equation:

$$\frac{CaIII}{CaII} = \frac{\gamma + C * n_e}{\alpha * n_e} \quad (5)$$

where C and α are the collisional ionization coefficient and radiative recombination coefficient respectively, and γ is the photoionization rate. The same equations could be written for the sodium equilibrium, by replacing CaII by NaI, and CaIII by NaII. Calcium depletion has been determined in the Sun vicinity by using the NaI/CaII ratios towards nearby stars (Bertin et al.

1993a). This measurement is made possible by the absence of sensitivity of the NaI/CaII ratio to the electron density when the temperature is around 7500K, as shown by Pottasch (1972). This temperature is indeed the most likely value for the Local Cloud and its very close companion (or its extension) which moves at a slightly larger velocity called the G cloud (see LBFVB). These calculations use the above calcium equilibrium and the corresponding equilibrium between the two dominant forms of sodium, i.e. NaI and NaII. When measured, the NaI/CaII ratio roughly varies between 0.09 and 0.25 for gas at the LIC or G velocities, as found for targets within 25 pc, with the most likely value for the LIC being 0.19 from αPeg. This is detailed in the Appendix. This small value is in agreement with the results of Welsh et al (1991) for all stars with N(NaI) $\leq 10^{11}$ cm^{-2}. The corresponding calcium depletion was found to be δ(Ca) = δ(Na) -1.0 (resp. 1.3) if R=NaI/CaII=0.10 (resp. 0.20). Using the sodium depletion range δ(Na) = -0.6 $\pm$ 0.3 of Phillips, Pettini and Gondalekhar (1984), this resulted in δ(Ca) = $-1.6^{+0.3}_{-0.3}$ (resp. $-1.9^{+0.3}_{-0.3}$) if NaI/CaII = 0.1 (resp. 0.2).

The way the Bertin et al. (1993a) calculations were done has the following consequence: provided the same ionization and recombination coefficients are used, it is equivalent to use simultaneously the CaII column, the calculated depletion and the calcium equilibrium equation, or to use simultaneously the NaI/ CaII ratio, and the sodium equilibrium equation. In other words, the same result would be obtained through the method described at the beginning of this section, or by converting the CaII column into an NaI column through the mean NaI/CaII ratio and write the sodium equilibrium. We will choose the second method, since uncertainties are more easily estimated in this way. The CaII column-density to δ Cas has been measured by Lallement and Bertin (1992), and found to be 0.5 $\pm$ 0.10 10^{+10} cm^{-2} (The error bar has been reestimated using profile fitting, and found to be about a factor of two lower than the initially quoted error). It follows from

$$R = \frac{NaI}{CaII} = 0.19^{+0.06}_{-0.10} \text{ that :}$$
$$N_{NaI} = N_{CaII} * R = 0.095^{+0.055}_{-0.059}\, 10^{10} \text{ cm}^{-2} \quad (6)$$

On the other hand:

$$N_{Na} = N_H * 10^{\delta(Na)} * (Na/H)_{SUN}$$
$$= 1.8\, 10^{18} * \frac{1}{1-f} * 1.9\, 10^{-6} * 10^{-0.6\pm0.3} \quad (7)$$
$$= 0.86^{+0.86}_{-0.43}\, 10^{12} * \frac{1}{1-f}$$

using the sodium abundance of Ross and Aller (1976). The equilibrium of sodium can be written as:

$$Na_{II}/Na_I \simeq Na/Na_I = \frac{\gamma_{Na} + C_{Na} * n_e}{\alpha_{Na} * n_e} \quad (8)$$

Here we will make use of the same coefficients as in Bertin et al (1993a). γ is taken from Péquignot and Aldrovandi (1986) and calculated for the UV field of de Boer et al. (1973), resulting in γ(Na)= $1.30^{+0.2}_{-0.3}$ 10^{-11} s^{-1}. Here the uncertainty has been derived from the work of Pequignot and Aldrovandi (1986) who have calculated γ for four radiation fields available from litterature and find the above range. α (Na) and its temperature dependence are from Seaton (1951, 1962), α equals 0.23 10^{-12} cm^3 s-1 at T=7500 K. The collisional ionisation rate and its temperature dependence is taken from Seaton (1962) who calculated C(Na) = 1.30 10^{-11} cm^3 s-1. For more details see Bertin et al. (1993a). Eq. (8) becomes:

$$Na/NaI = (1.3^{+0.2}_{-0.3}10^{-11}/0.2310^{-12})(1 + n_e)/n_e =$$
$$Na/NaI = 56. * (1.00^{+0.15}_{-0.23} + n_e)/n_e \quad (9)$$

Combining with (6) and (7):

$$900.^{+3900.}_{-600.} * \frac{1}{1-f} = 56.(1.00^{+.15}_{-0.23} + n_e)/n_e \quad (10)$$

In case the ionization degree is assumed to be negligible then f$\simeq$ 0, and n_e is found from (10) to be equal to 0.07 (-0.06,+0.21) cm^{-3}. This shows a posteriori that this assumption is not really valid because for almost the whole resulting interval n_e is of the order of the neutral H density. If searching for a general solution, one needs to express f as a function of n_e and n(HI), and thus make some assumption on the neutral H density. The neutral H density measured inside the heliosphere is n(HI) $_{hel}$= 0.06-0.15 cm^{-3}, with the most likely value being around 0.1 cm^{-3} (see a last measurement and a review in Quémerais et al., 1994). The resulting neutral H density just outside the heliosphere is depending on the neutral filtration factor at the heliospheric interface (e.g. Baranov and Malama, 1993), itself a function of the electron density. For a plasma density of 0.1 cm^{-3}, the H density is reduced by about a factor of 2 inside the heliosphere, and by a factor of three when n_e=0.2 cm^{-3}. An approximate relation can be derived from the models of Baranov and Malama (1995) under the form: n(HI) $_{LIC}$= n(HI) $_{hel}$ * (3.2 -2.2 exp-(5.62*n_e)). Then approximately:

$$\frac{1}{1-f} = \frac{(n_{HI}+n_e)}{n_{HI}}$$
$$= 1 + \frac{n_e}{n_{HI,hel}*(3.2-2.2exp-(5.62*n_e)} \quad (11)$$

Combining this expression with the sodium equilibrium equation above, the electron density can be estimated for any heliospheric density. The results are displayed in Fig. 3.

The error interval for the electron density is large, because we have considered the cumulative effects of the uncertainties, and because we have been very conservative in quoting the errors on the sodium depletion and the NaI/CaII ratios. At 7000K, the interval for n_e= 0.05 (-0.04, +0.14) cm^{-3}. Nevertheless, this result gives a second indication that the electron density in the LIC is not negligibly small, and on the contrary is probably of the same order than the neutral H density. It is also interesting to note that at T= 7000K the two determinations have the common interval 0.14-0.19 cm^{-3}. However, the most probable electron density is found to be smaller by a factor of four than the value derived from magnesium equilibrium, and this certainly deserves further attention.

The same type of calculation can also be applied to the Altaïr component (Lallement et al., 1995a) at the LIC Doppler shift.

However, because the LIC and the G cloud Doppler shifts are too close to allow the distinction between the two clouds, we do not know which one of them creates the absorption lines at this wavelength. For this component, CaII, NaI and MgII (or FeII) amounts are available at the same time. N(MgII) = 5.3 10^{12} cm^{-3} is slightly smaller than for δ Cas, while N(CaII) = 0.7 10^{10} cm^{-3} (Lallement and Bertin, 1992) is somewhat larger. These column-densities are less precisely derived than for δ Cas, because the Altair components are blended. As a consequence, we discuss mean values only. From the NaI column (Ferlet & al. 1986), and assuming the same magnesium abundance as towards Capella, one gets in the same way as for δ Cas n_e(Altair) = 0.08 cm^{-3} as an approximate value. If instead of the LIC, the G cloud is seen in absorption towards Altair, then the magnesium abundance is four times larger, as derived towards αCen by Linsky and Wood (1996), and the resulting approximate value for the electron density is about four times smaller, i.e. 0.02 cm^{-3}, for the same depletion of sodium, or slightly more if the sodium is, as for the magnesium, less depleted than towards δCas (but the dominant effect will remain the large depletion of the magnesium). This shows that if the G cloud is detected towards Altair, then we have an indication from the sodium ionization that it is characterized by a smaller plasma density.

5. Conclusions

The GHRS Echelle-B spectra of the star δ Cas around the MgII and MgI lines provide a new measurement of the MgII/MgI ratio in the solar environment. The found ratio R$\simeq$ 400 is a factor of $\simeq$2 higher than the ratio measured towards Sirius, maybe a sign of inhomogeneity in the Local Cloud, i.e. a temperature, density or ionization gradient, although better measurements are necessary to confirm this discrepancy. When assuming an homogeneous LIC temperature of 7000K, equilibrium conditions between photoionization and dielectronic recombination, and taking into account the charge-exchange between the neutral magnesium and the protons, such a ratio implies an electron density of n_e = 0.28 (-0.14,+0.34) cm^{-3} on the path to δ Cas. The similarity of the resolved LIC column-densities of FeII and MgII towards Capella, G191-B2B, δ Cas and Altaïr on one hand, and of the LIC CaII columns towards the angularly close δ Cas, α Aql, α Cep, and α Lac allows an estimate of the neutral H column-density towards δ Cas by comparison with Capella (Linsky et al., 1992). In turn, the combination of the neutral H column with the LIC CaII and NaI column-densities measured from ground allows to calculate the NaII/NaI ratio, and to estimate the electron density from the sodium ionization balance. The resulting electron density is n_e= 0.05 (-0.04, +0.14) cm^{-3} towards δ Cas. An approximate value for the electron density towards Altaïr is derived in the same way aand found to be about 0.08 cm^{-3} if the sampled medium has the LIC magnesium abundance, and about 0.02 cm^{-3} if the G cloud, instead of the LIC, is detected in this direction.

There is a rather large discrepancy between the most probable electron densities, as they come out from magnesium and sodium/calcium equilibrium respectively, in case of δ Cas. The sodium/calcium-derived most probable plasma density is a factor of 5 smaller as compared with the magnesium determination. At the same time, the error bar on the sodium/calcium determination is larger due to uncertainty on the sodium depletion and the LIC NaI/CaII ratio. New measurements of the latter parameter should help to reduce these uncertainties. The sodium/calcium results confirm that the ionization degree is significant in the local cloud, but, in spite of the existence of a common interval between the two density ranges $n_e \simeq$ 0.14-0.19 cm^{-3}, the discrepancies between the two determinations may reveal either systematic errors, as the use of uncorrect ionization or recombination coefficients, the neglect of one physical phenomenon, or the actual departure from ionization equilibrium. The sodium/calcium upper limit of 0.19 cm^{-3} is consistent with the upper limit one can derive from the minimum distance to the solar wind termination shock (60 AU) presently implied by the Voyager and Pioneer observations. The density based on the magnesium equilibrium is close to the circumsolar value of about 0.25 cm^{-3} derived by Frisch (1994) from Anomalous Cosmic Rays abundances. However, this last value if found by assuming the absence of filtration of neutral oxygen and carbon at the heliospheric interface, or the same filtration for both species. If there is a significant difference between the filtrations for the two species, some correction to this value is necessary. Calculations of the neutral oxygen coupling with the plasma have been done by Fahr et al. (1995) and Izmodenov et al. (1996), showing that oxygen may decrease by a factor of 2. This will lower by approximately the same factor the derived density (leading to 0.12 cm^{-3} or less), if carbon is not filtered. But the same calculations for carbon are still missing. The lower range of the common interval (about 0.14 cm^{-3}) is marginally compatible with the electron density range of 0.05-0.10 cm^{-3} derived from the interstellar H deceleration at the heliospheric interface according to the Baranov and Malama (1993) model results (Lallement et al. 1993). The central value deduced from calcium (0.05 cm^{-3}) is only slightly smaller than the minimum value from the H deceleration. It is also in rather good agreement with the moderate hydrogen ionization degree (e.g. 20% if n_e = 0.05 cm^{-3} and N(HI) = 0.20 cm^{-3}) which local EUV sources could maintain (Vallerga and Welsh, 1995), as well as with the 25% helium ionization mesured by Vennes et al. (1993) towards GD246 and the HI/HeI ratio of about 14 measured by Dupuis et al. (1995). New data, involving equilibria of other species appear to be necessary to bring better constraints on the ionization states in the surrounding medium and provide better predictions on the future crossing of the termination shock by the deep space probes.

Appendix A: NaI/CaII ratios for the LIC and the close G cloud

There are four unambiguous measurements for the G clouds: 0.09 (-0.03,+0.04), 0.10 (-0.08,+0.15), 0.13 (-0.04,+0.19), 0.26 (-0.08,+0.12) (for ι Cen, τ^3Eri, HR4023, λSco), one ambiguous (e.g. LIC or G) ratio of 0.17 (Altair), five upper limits of 0.26, 0.20, 0.25, 0.19, 0.20 (resp. α Cep, τ^3Eri, γAqr, δHer, αLac) in unambiguous LIC cases but very low amounts of material,

and one LIC and G blend (αPeg, see below) giving a ratio of 0.19 (-0.09,+0.17). We have excluded targets with NaI column-densities in excess of 10^{10} cm^{-2} to avoid blending with other components than G or the LIC. As it can be seen, there are no cases where a well-defined NaI absorption is unambiguously due to the LIC and only the LIC. However, there are strong arguments in favor of a LIC NaI/CaII ratio of the same order as the one measured for the G cloud: 1)- the G cloud is extremely close, has a temperature, a velocity, and probably a density of the same order and suffers the same ionizing field as the LIC (being so close). Differences between its NaI/CaII ratio and the LIC ratio in these conditions should be attributed to gazeous calcium abundance variations only, and then to a real different history, because for T=5000-15000K, the ratio is almost insensitive to the electron density. Whatever the G cloud density, there are no reasons for its NaI/CaII, ratio to be very different. 2) The LIC NaI/CaII ratio has been "indirectly" measured in the particular case of α Peg. For this star, the NaI line has been detected, but as show the most recent CaII data, the detected absorption is a blend of two lines, corresponding to two clouds of equal CaII column-densities, one of them being the LIC. As discussed in Bertin et al. (1994), the NaI line center is exactly at the median velocity between the two clouds locations, implying similar NaI amounts in both blended lines, and then similar NaI/CaII ratios. One then can calculate this ratio, which is found to be 0.19 (-0.09,+0.17). As a conclusion, it is extremely likely that the LIC ratio is comprised between 0.1 and 0.2, in agreement with the G cloud ratio. In the calculations of Sect. 4, we have used the slightly larger interval R = 0.09-0.25.

References

Aldrovandi S.M.V., Péquignot D., 1973, A&A, 25, 137.

Allan R.J., Clegg R.E.S., Dickinson A.S., Flower D.R., 1988, M.N.R.A.S., 235, 1245.

Axford W.I., 1990, in Physics of the outer Heliosphere, ed. E. Page and S. Grzedzielski, Cospar Coll. Series, Pergamon, Vol 1

Baranov V.B., Malama Ju. G., 1993, J. Geophys. Res., 98, 15157

Bertin P., Lallement R., Ferlet R., Vidal-Madjar A., 1993a, A&A, 278, 549

Bertin P., Lallement R., Ferlet R., Vidal-Madjar A, 1993b, J. Geophys. Res., 98, A9, p 15193.

Bruhweiler F.C, Oegerle W., Weiler E., Stencel R., Kondo Y.,1984, in Local Interstellar Medium, ed. Y. Kondo, F.C. Bruhweiler, B.D. Savage, (NASA CP-2345), p64

Bruhweiler F.C, Oegerle W., Weiler E., Stencel R., Kondo Y., 1984, in Future of ultraviolet Astronomy Based on Six Years of IUE Research, ed. J. Mead, R. Chapman, Y. Kondo (NASA CP-2349), p200

Cheng K.P., Bruhweiler F.C., 1990, ApJ., 364, 573

Cox D. P., Reynolds R.J., 1987, Ann. Rev. Astr. Ap., 25, 303

Duncan D.K., 1992, Goddard High Resolution Spectrometer Instrument Handbook Version 3.0 (Space Telescope Science Institute)

Dupuis J., Vennes S., Bowyer S., Pradhan A., Thejll P., 1995, ApJ., 455, 574

Fahr H.J., Osterbart R., Rucinski D., 1995, A&A, 394, 587

Ferlet R., R. Lallement, A. Vidal-madjar, 1986, A&A, 163, 204

Frisch P.C., 1981, Nature, vol 293, 377

Frisch P.C., D.G. York, 1983, ApJ, 271, L59

Frisch P.C., D.G. Welty, D.G. York, J.R. Fowler, FWYF, 1990, ApJ, 357, 514

Frisch P.C., 1994, Sci, 265, 1443

Genova R., Molaro P., Vladilo G., Beckman J.E., 1990, ApJ, 355, 150

Hobbs, 1969, ApJ, 157, 135

Hobbs L. M., Welty D.E., 1991, ApJ, 368, 426 Ip W.H., Axford W.I., 1986, Adv. Space Res., 6, 27

Izmodenov V., Malama J., Lallement R., 1996, A&A, in press

Jacobs V.L., Davis J., Rogerson J.E., and Blaha M., 1979, Ap. J. 30, 627

Lallement R., A. Vidal-madjar, R. Ferlet, 1986, A&A, 168, 225

Lallement R., Bertin P., (LB), 1992, A&A, 266, 479

Lallement R., Bertaux J.L., Clarke J.T., 1993, Science, 21 Mai

Lallement R., R. Ferlet, A. Vidal-Madjar, C. Gry, 1990, in Physics of the Outer heliosphere, (Varsovie, Sept 89) COSPAR COLLOQUIA SERIES, VOL 1, ed. by S. Grzedzielski and D. E. Page, Pergamon

Lallement R., P. Bertin, R. Ferlet, A. Vidal-Madjar, J.L. Bertaux, 1994, LBFVB, A&A, 286, 898

Lallement R., R. Ferlet, A.M. Lagrange, Lemoine M., A. Vidal-Madjar, 1995, A&A, 304, 461

Landsman W.B., Murthy J., Henry R.C., Moos H.W., Linsky J.L., Russel J.L., 1986, ApJ, 303, 791

Lemoine M., Vidal-Madjar A., Ferlet R., Bertin P., Gry C., Lallement R., 1996, A&A, 308, 601

Linsky J.L., Brown A., Gayley K., Diplas A., Savage B.D., Ayres T.R.,Landsman W., Shore S.N., Heap S.R., 1993, ApJ, 402, 694

Linsky J.L., A. Diplas, B.E. Wood, A. Brown, T. R. Ayres, Savage B.D., 1995, ApJ., 451, 335

Linsky J.L., Wood B.E., 1996, ApJ, 463, 254

McClintock W., Henry R.C., Linsky R.C., Moos H.W., 1978, ApJ, 225, 465

Molaro P., Vladilo G., Beckman J.E.,1986, A&A, 161, 339.

Morton D.C., 1991, ApJ Suppl. Series, 77, 119

Murthy J., Henry R.C., Moss H.W., Landsman W.B., Linsky J.L., Vidal-Madjar A., Gry C., 1987, ApJ, 315, 675

Nussbaumer H., Storey P.J., 1986, A&A Suppl. Ser., 64, 545

Osterbart R., Fahr H.J., 1992, A&A, 264, 260

Pequignot D., Aldrovandi S.M.V., 1986, A&A, 161, 169

Phillips A.P., Gondhalekar P.M., Blades J.C., 1981, M.N.R.A.S., 195, 485

Phillips A.P., Pettini M., Gondalekhar P.M., 1984, MNRAS, 206, 337

Pottasch S.R.,1972, A&A, 20, 245

Quemerais E., Bertaux J.L., Sandel B.R., Lallement R., 1994, A&A, 290, 941

Reynolds R.J., 1987, ApJ, 323, 118

Reynolds R.J., 1990, ApJ, 348, 153

Ross J.E., Aller L.H., 1976, Sci, 191, 1233

Seaton M.J., 1951, MNRAS, 111, 368

Seaton M.J., 1962, Atomic and Molecular Processes, Ed D.R. Bates, Academic Press, NY.

Slavin J.D., 1989, ApJ, 346, 718

Vallerga J.V., Vedder P., Welsh B.Y., 1993, ApJ, 414, L65

Vallerga J.V., Welsh B.Y., 1995, ApJ, 444, 202

Vennes S., Dupuis J., Rumph T., Drake J., Bowyer S., 1993, ApJ, 410, L119

Vidal-Madjar A., Laurent C., Bruston P., Audouze J., 1978, ApJ, 223, 589

Welsh B.Y., Vedder P.W., Vallerga J.V., Craig N., 1991, ApJ, 381, 462

Witte M., H. Rosenbauer, M. Banaszkiewicz, H.J. Fahr, 1993, Adv. Space Res., N° 6, Vol 13, p 121